CYCLE 3 FOS RED SIDE SUPER-FLATS

D. Lindler, R. Bohlin, and C. Keyes

FOS Instrument Science Report CAL/FOS-134
January 26, 1995

ABSTRACT

A new set of FOS flat fields are available for correcting pre-Costar red side single aperture observations. The flats are computed using the "super-flat" technique (Lindler, et al. 1993) on observations of WD0501+527 taken on Nov. 25 and 26, 1993 (Proposal 5229). Application of the files to standard star observations taken before 1994 indicate that the new flat field files should be used for reprocessing single aperture data for gratings H19, H27, and L15 taken after August 7, 1992, and single aperture data for gratings H40, H57, L65, and the prism after June 18, 1992. The 1 to 2 percent ringing seen in the results for proposal 2821 from June 1992 is not present in these new results.

INTRODUCTION

The super-flat technique requires multiple observations of a star in the 4.3 arcsec aperture. Moving the star in the X (dispersion) direction moves spectral features to a different photocathode position in the observed data. Detector granularity features will not move. To separate the spectral flux distribution from the FOS flat field granularity, we create a non-linear system of equations.

Let: C(i) be the unknown count rate spectrum
F(i) be the unknown flat field vector

We observe the star at different X locations in the 4.3 arcsec aperture to obtain m observations (O1, O2, ..., Om) with the spectral features shifted by Ki data points between observation 1 and observation i.

$$
\begin{aligned}
O1(i) &= F(i) * C(i) && i=1,n \\
O2(i) &= F(i) * C(i+k2) && i=1,n \\
O3(i) &= F(i) * C(i+k3) && i=1,n \\
&\ldots \\
Om(i) &= F(i) * C(i+km) && i=1,n
\end{aligned}
$$

For our case (proposal 5229), n is 2064, m is 7 and the maximum shift between any two observations is 36 pixels. This leads to a over-determined system of 7 x 2064 (14448) equations with only 2n + 36 (4164) unknowns. An iterative method for solving this system is described in Lindler, et al. 1993.

OBSERVED DATA

The FOS was used to observe WD0501+527 (G191B2B) at 7 locations in the 4.3 arcsec aperture using the red detector and seven dispersion modes (H19, H27, H40, H57, L15, L65, and the prism) on November 25-26, 1993 (Cycle 3 proposal 5229). Unlike the earlier superflat data taken by proposal 2821 (March-July, 1992), this new data used unequal offsets in the 4.3 arcsec aperture. These offsets (listed in table 1) were derived to avoid the ringing present in the 2821 results.

TABLE 1

X-Offsets from the center of 4.3 arcsec aperture (arcsec)	Corresponding pixel shift in data points (1/4 diode units)
-1.464	-19
-0.925	-12
-0.385	-5
0.000	0
0.077	1
0.231	3
1.310	17

All observations were taken with the default XSTEPS=4 and OVERSCAN=5.

RESULTS:

Figures 1 to 7 show the computed stellar count rate spectra for each dispersion mode. The estimated one sigma uncertainty in the mean (in percent) is plotted below each spectrum. This uncertainty is computed from the scatter of the seven computed count rate vectors, C(i), from their average. None of the plots show the ringing that was present in the earlier analysis of the proposal 2821 data.

Figures 8 to 14 show the average flat field response for each dispersion mode along with the one sigma scatter about the average. Regions with abnormally large sigmas indicate blemishes which change from one observation to the next.

Figures 15 through 21 show a comparison of the new super-flat with the flats used by the Routine Science Data Processing System (RSDP) after the dates in Table 2. The top plot shows the flat field used by RSDP for all data currently in the Archive after the applicable date in Table 2 for the improved flats. In some cases, RSDP used a different flat field file for the C-2 aperture (0.25 arcsec slit). These special C-2 flats are shown in the second plot position from the top. The third position shows the new superflat that is now available for

improved reprocessing of old data. The recommended use after dates shown in the titles of the superflats are determined by visual inspection of between 20 to 40 standard star observations for each dispersion mode taken during cycles 1-3. The fourth plot position shows the cycle 4 flat field used by RSDP (Keyes, 1995). The cycle 4 flat fields are computed using the same super-flat technique. The bottom plot in Figures 15 to 21 shows the ratio of the original flat field used by RSDP to process all the currently archived spectra to the new cycle 3 superflats.

CONCLUSIONS AND RECOMENDATIONS

The new pattern for positioning the star in seven locations in the 4.3 arcsec aperture successfully avoids the ringing problem seen in the analysis of earlier data where a constant offset between positions was used. This pattern should be used for any new superflat observations.

We have visually compared the results of 20 to 40 standard star spectra for each dispersion mode (taken between November 1990 and December 1993) as calibrated with both the original RSDP flat fields and with the new superflats. Results indicate that for default re-processing, the new superflats should be used after the following dates:

TABLE 2

Dispersion Modes	Use-after date	End-Date
H19, H27, L15	7-AUG-1993	31-Jan-1994
H40, H57, L65, Prism	18-JUN-1992	31-Jan-1994

REFERENCES:

Lindler, D., Bohlin, R., Hartig G., and Keyes, C., 1993, FOS FLATS FROM SUPER SPECTRA, FOS Instrument Science Report CAL/FOS-088.

Keyes, C., 1995 in preparation.

FIGURE CAPTIONS

1-7) The average count rates for the spectra of WD0501+527 using the method described in this paper. Below each plot is the estimated one sigma uncertainty in the super spectrum.

8-14) The average flat-field granularity vector computed for each diserser mode. The one sigma scatter from the average is plotted beneath each granularity vector. The flat field is set to 1.0 where sharp changes in the detected count rate give poor flat field calibrations (eg. the prism above 4300 Angstroms and L65 between the 1st and 2nd orders).

15-21) A comparison of the new Cycle 3 super-flat with the previously used flat and current Cycle 4 RSDP flat fields. Up to five plots are shown for each dispersion mode. The first plot shows original RSDP flat field for the single apertures. If available, the flat for the C-2 aperture (0.25 arcsec slit) is shown in the second plot position. The third plot shows the new cycle 3 super-flat. The fourth plot shows the cycle 4 super-flats. The bottom plot shows the ratio of the new super-flat to the original single aperture flats (top plot). This bottom plot shows the amount of improvement to be expected from reprocessing data with the new super-flat for the time interval in Table 2.

Fig. 1

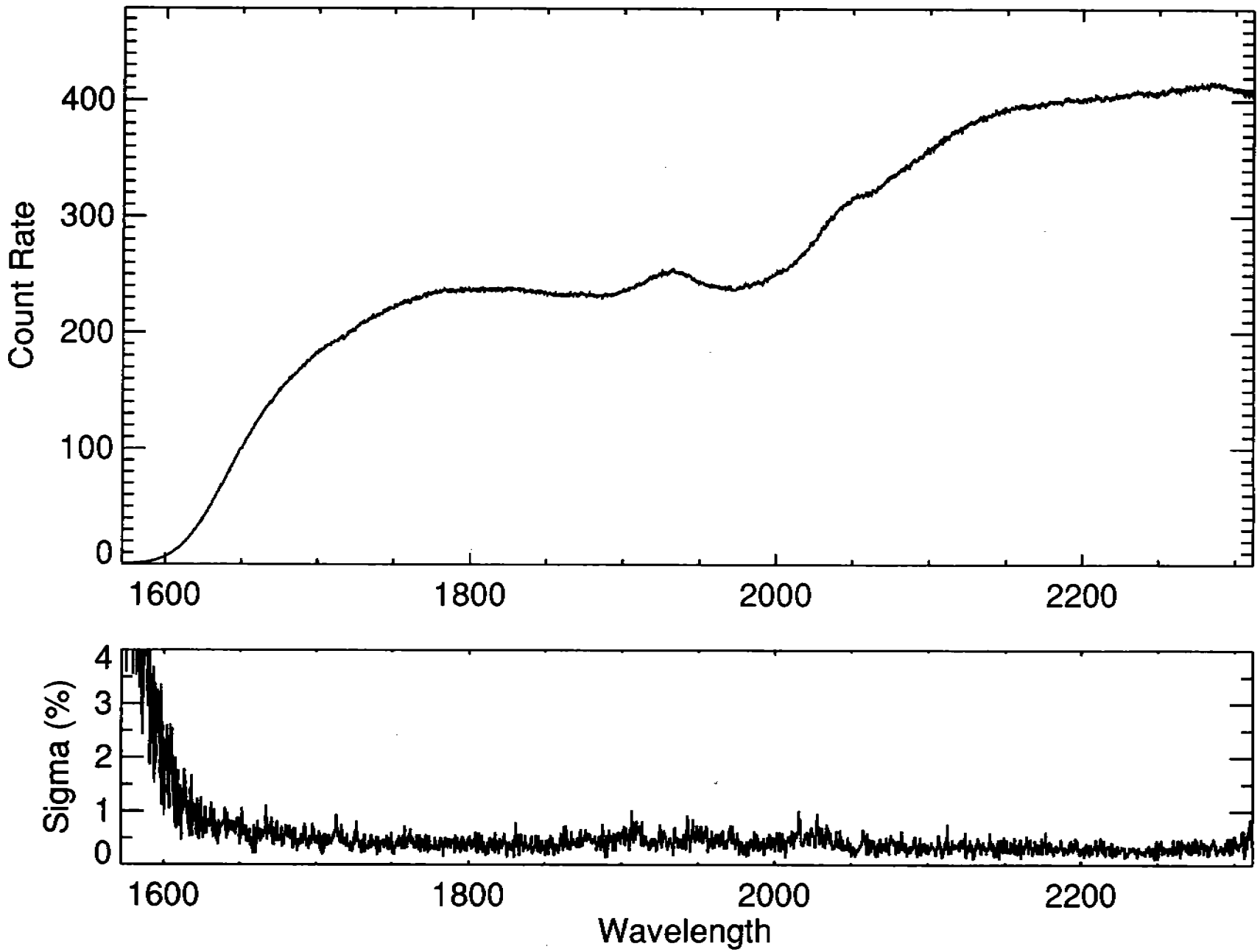
AMBER H19 WD0501+527
Count Rate
0
100
200
300
400
1600
1800
2000
2200
Sigma (%)
0
1
2
3
4
1600
1800
2000
2200
Wavelength

Fig. 2

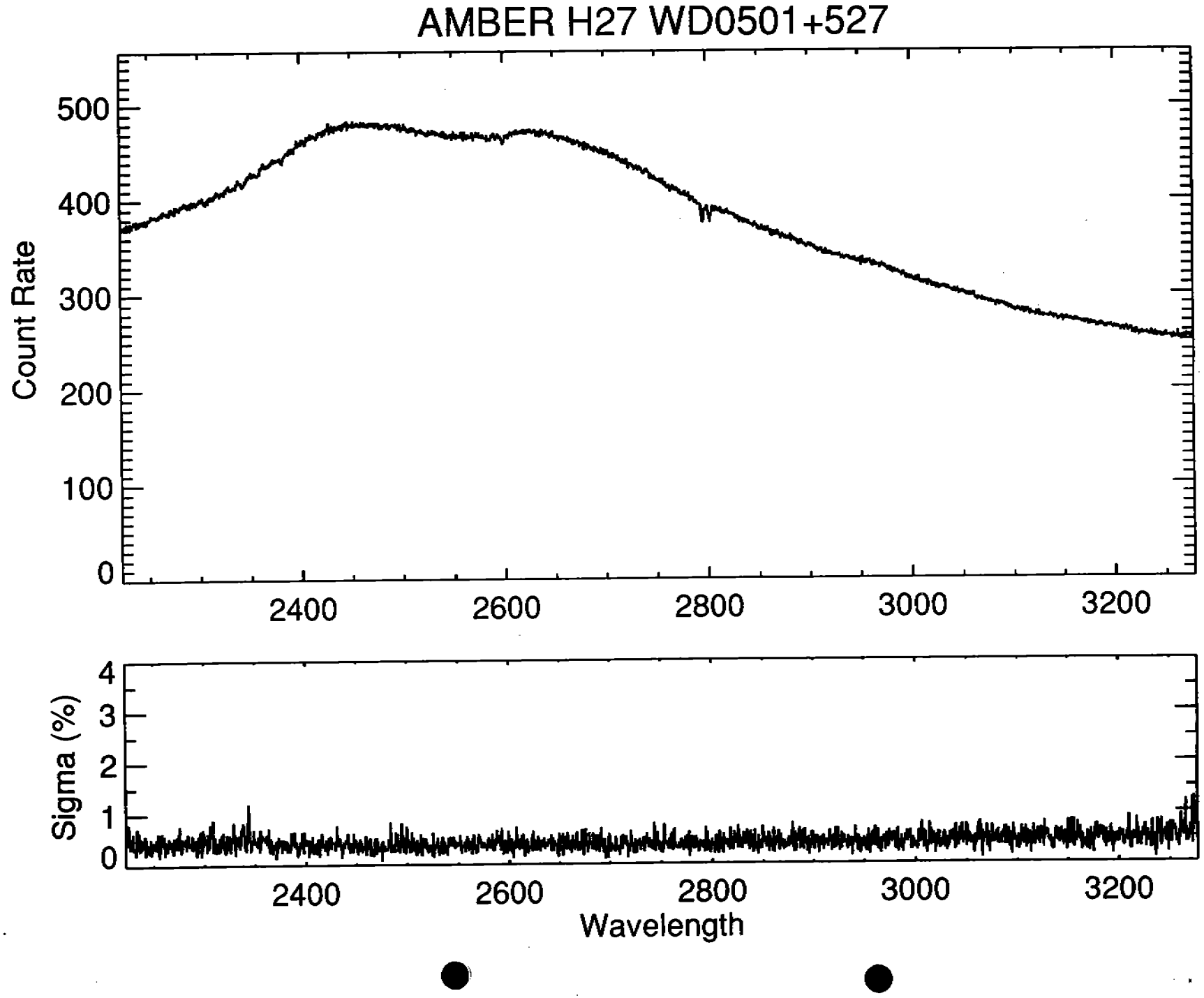
AMBER H27 WD0501+527
Count Rate
500
400
300
200
100
0
2400
2600
2800
3000
3200
Sigma (%)
4
3
2
1
0
2400
2600
2800
3000
3200
Wavelength

Fig. 3

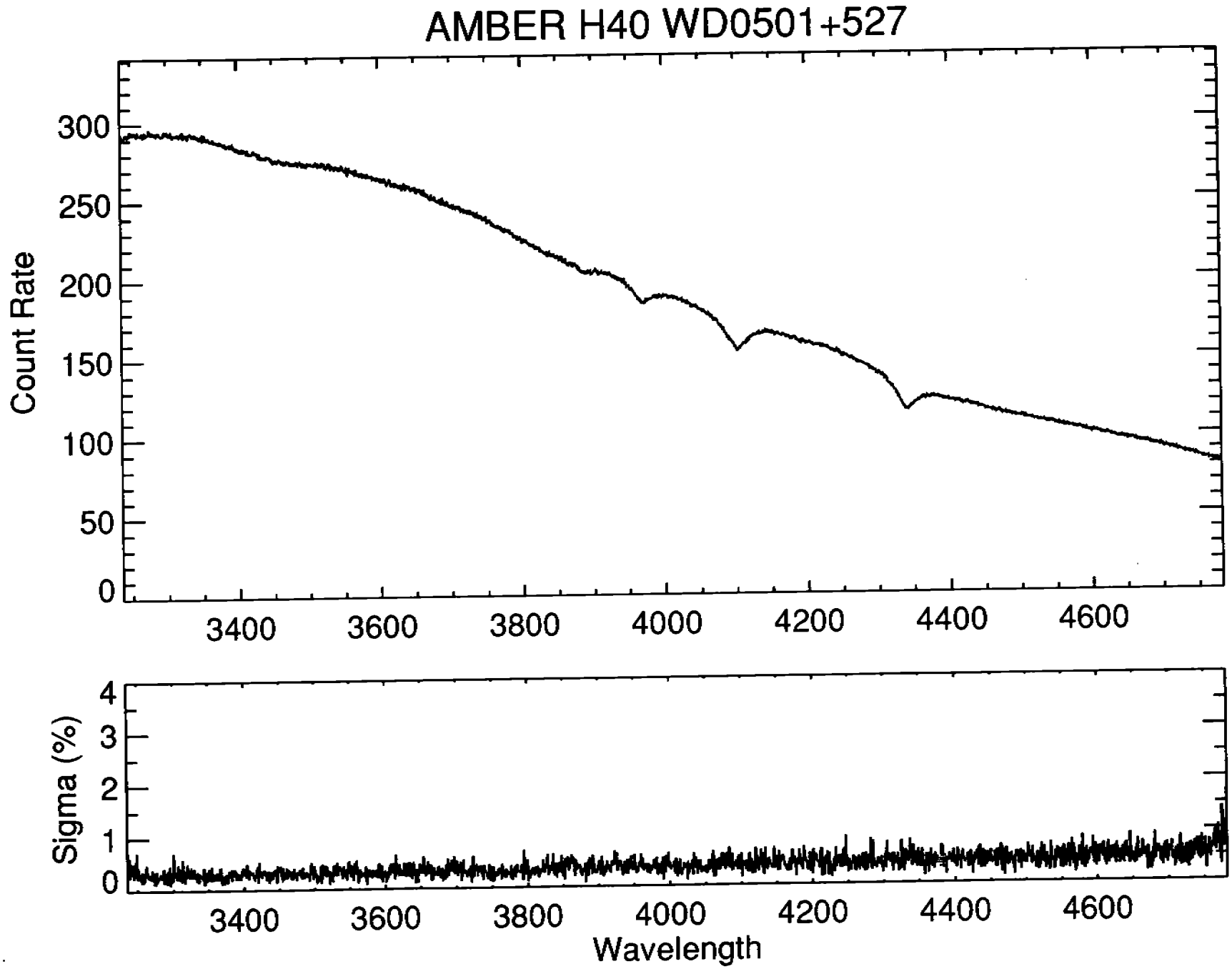
AMBER H40 WD0501+527
Count Rate
300
250
200
150
100
50
0
3400
3600
3800
4000
4200
4400
4600
Sigma (%)
4
3
2
1
0
3400
3600
3800
4000
4200
4400
4600
Wavelength

Fig 4

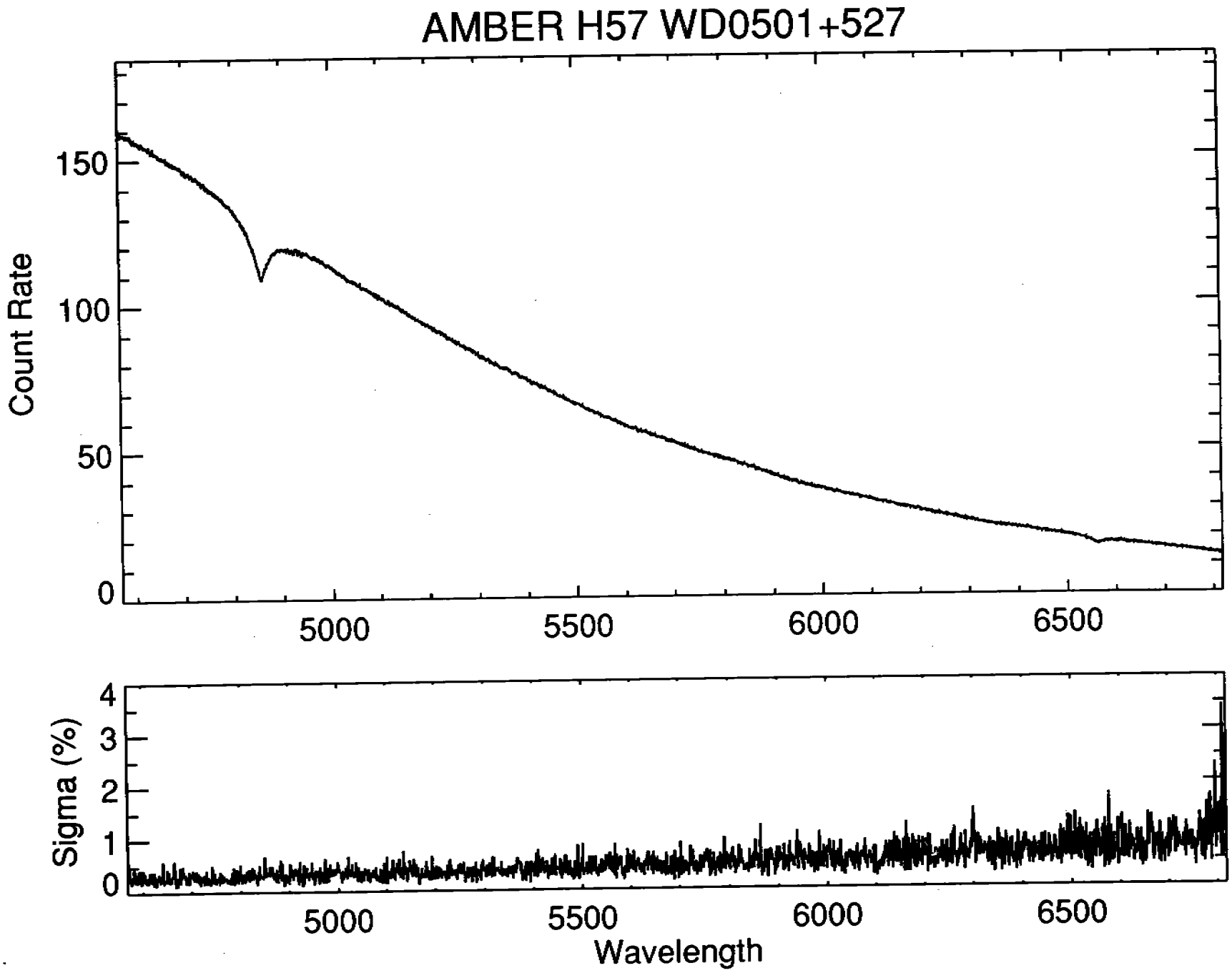
AMBER H57 WD0501+527
Count Rate
150
100
50
0
5000
5500
6000
6500
Sigma (%)
4
3
2
1
0
5000
5500
6000
6500
Wavelength

Fig. 5

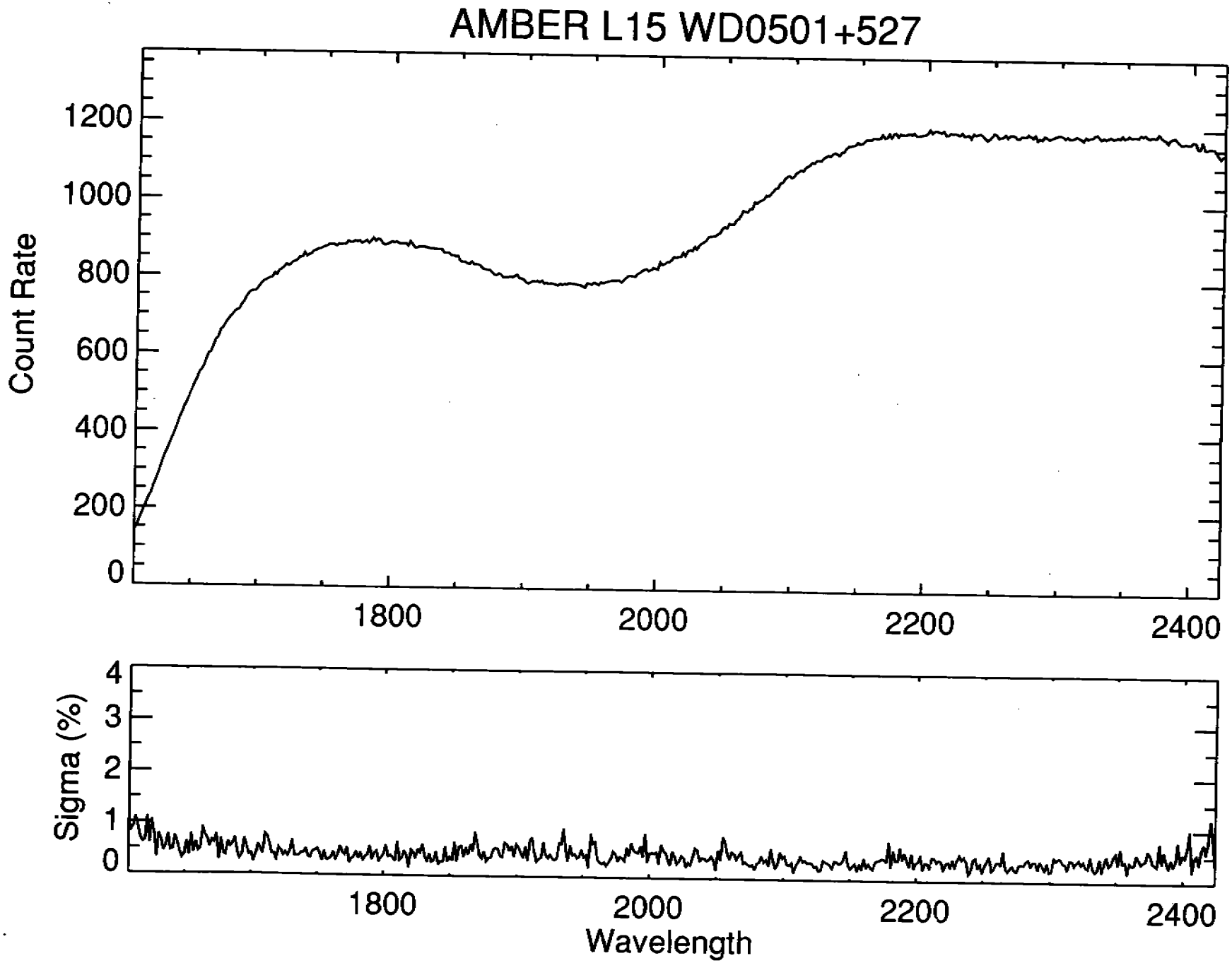
AMBER L15 WD0501+527
Count Rate
0
200
400
600
800
1000
1200
1800
2000
2200
2400
Sigma (%)
0
1
2
3
4
1800
2000
2200
2400
Wavelength

Fig. 6

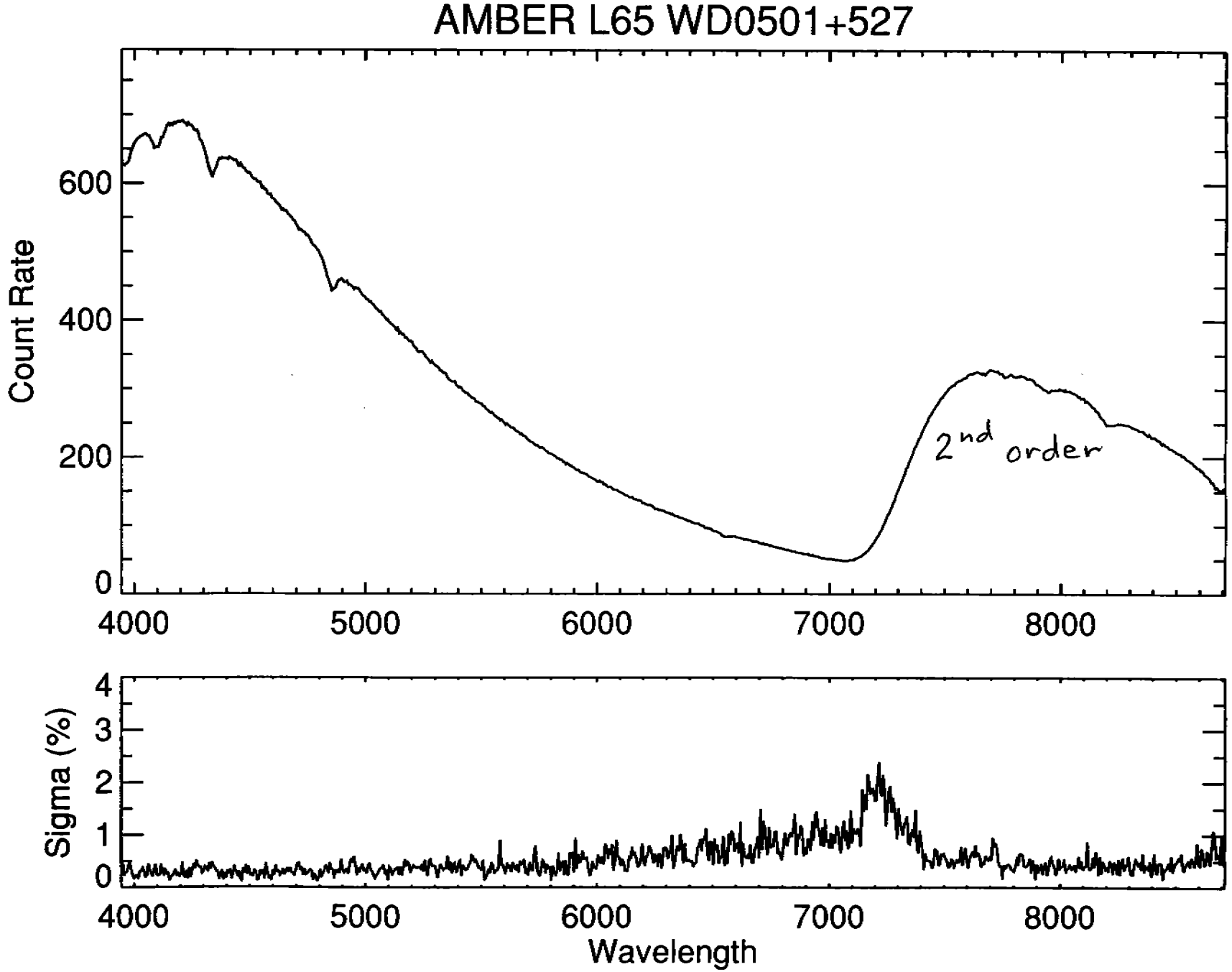
AMBER L65 WD0501+527
Count Rate
600
400
200
0
2nd order
4000
5000
6000
7000
8000
Sigma (%)
4
3
2
1
0
4000
5000
6000
7000
8000
Wavelength

Fig. 7

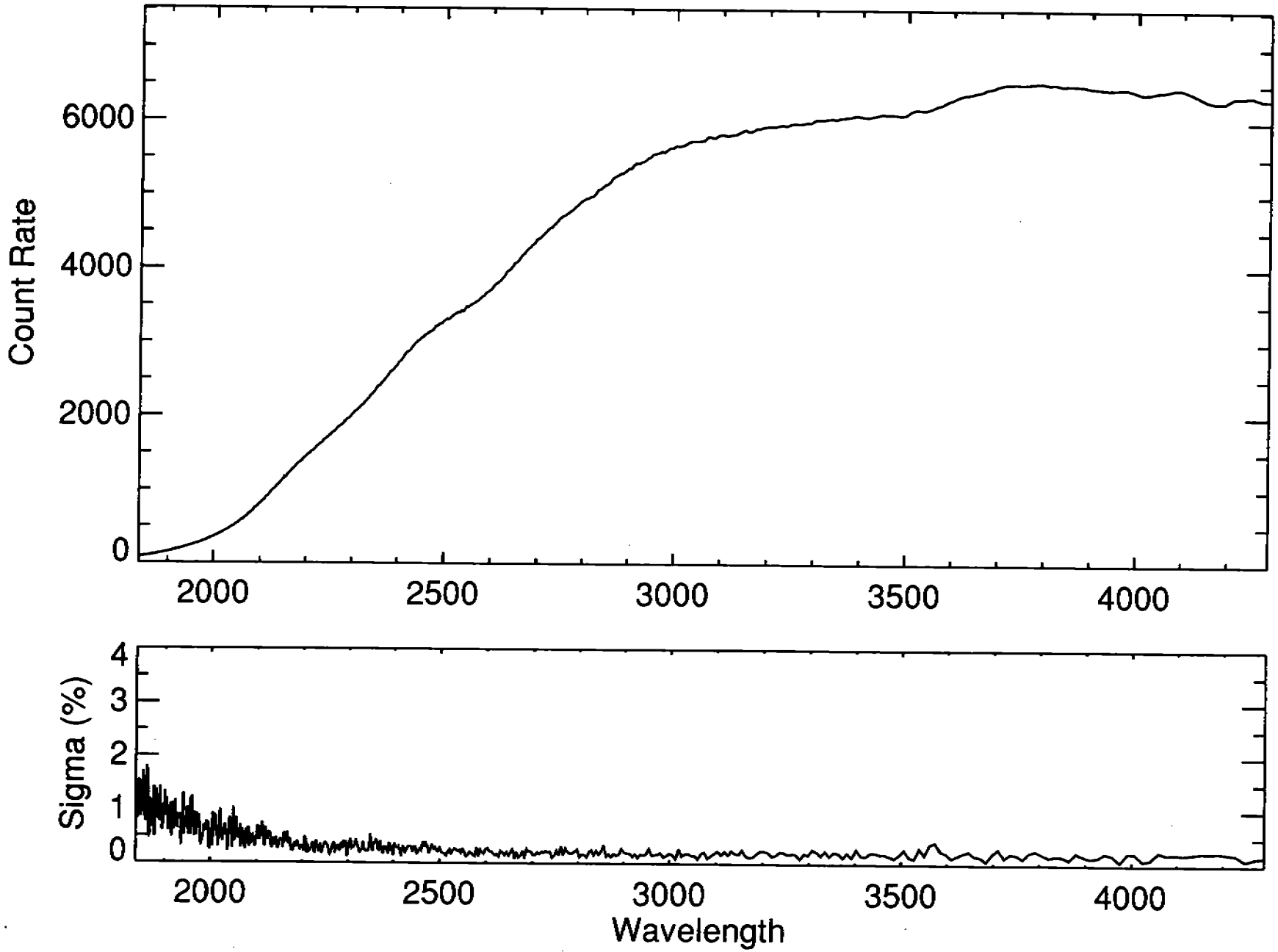
AMBER PRI WD0501+527
Count Rate
6000
4000
2000
0
2000
2500
3000
3500
4000
Sigma (%)
4
3
2
1
0
2000
2500
3000
3500
4000
Wavelength

Fig. 8

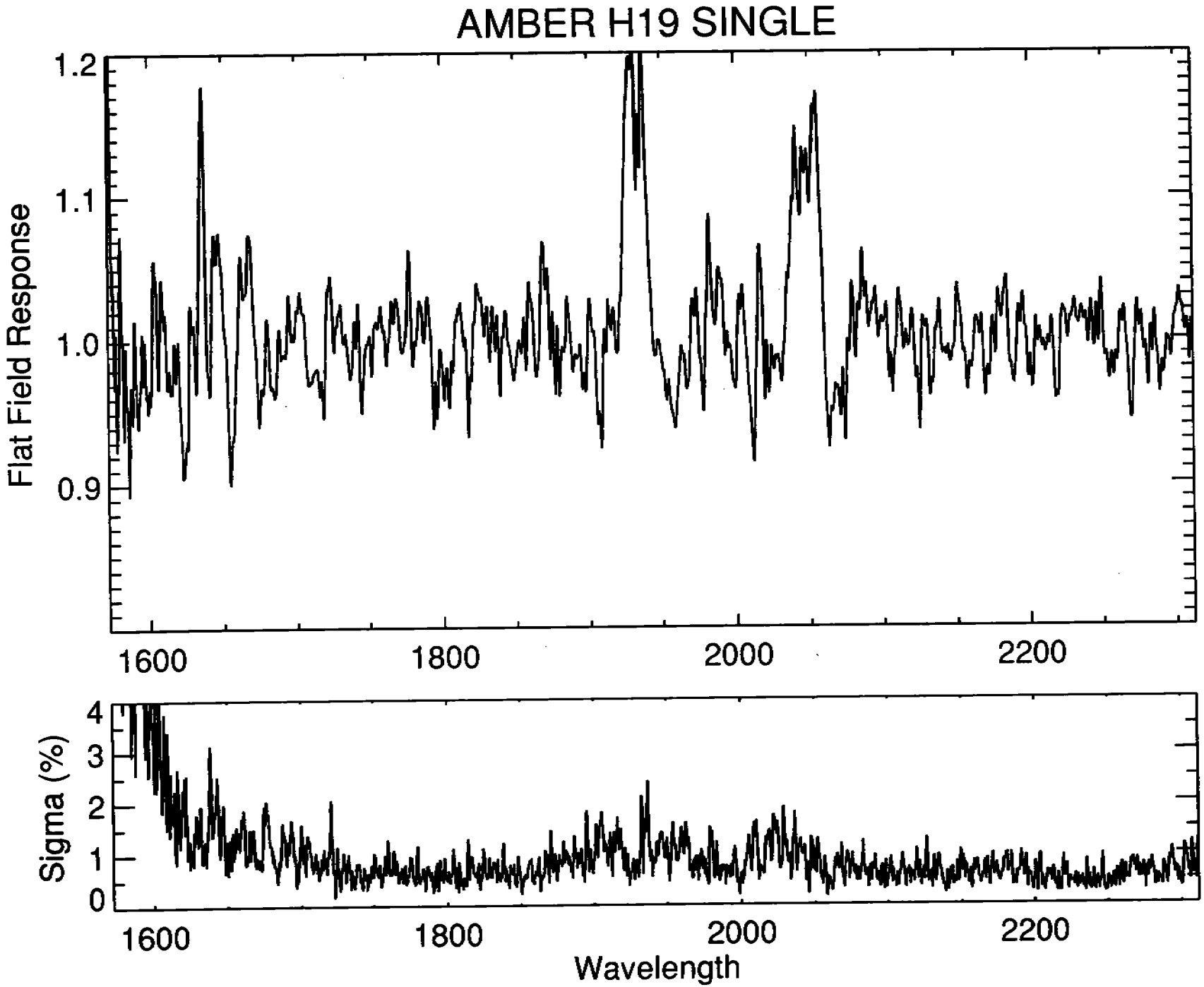
AMBER H19 SINGLE
Flat Field Response
1.2
1.1
1.0
0.9
1600
1800
2000
2200
Sigma (%)
4
3
2
1
0
1600
1800
2000
2200
Wavelength

Fig 9

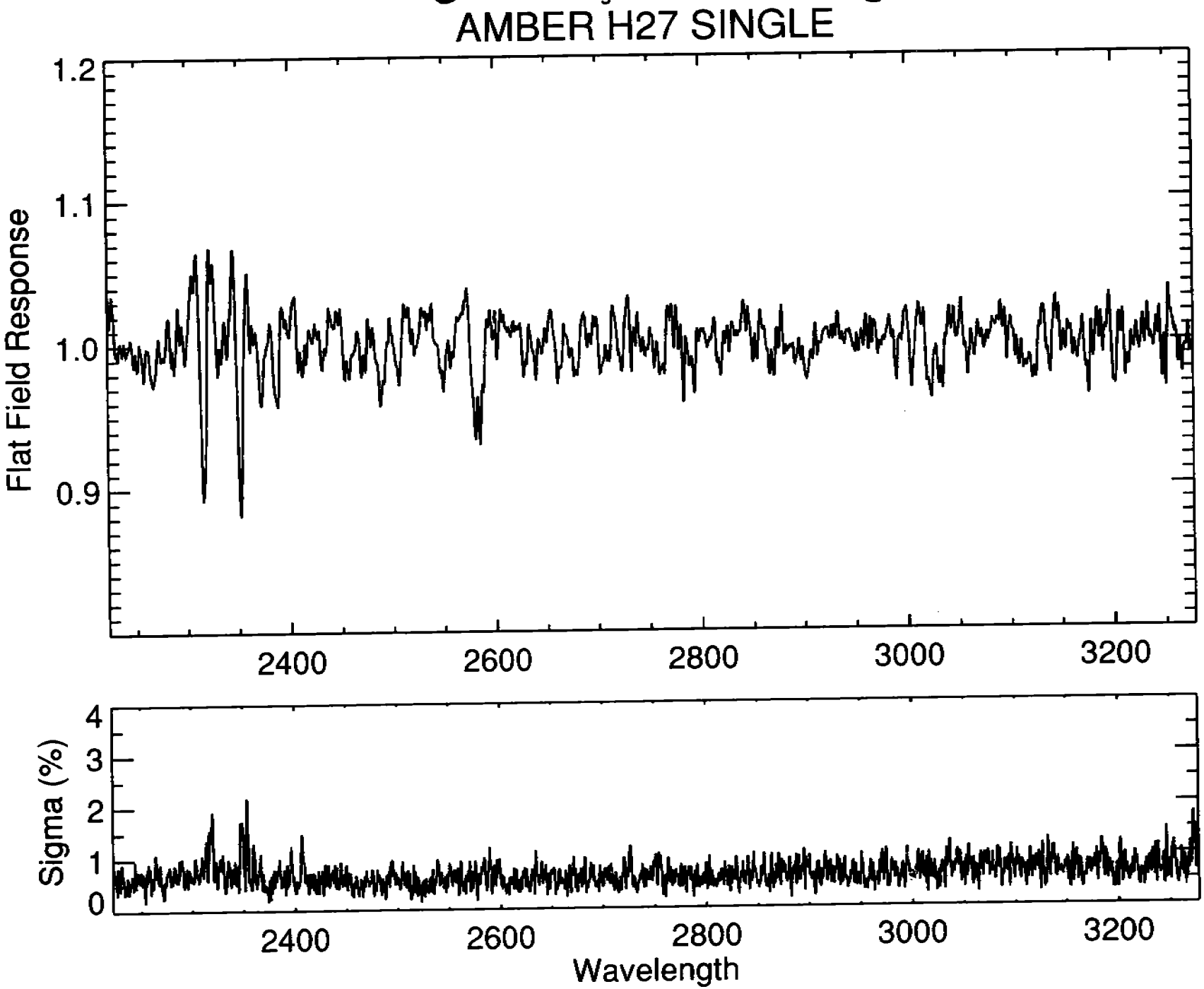
AMBER H27 SINGLE
Flat Field Response
1.2
1.1
1.0
0.9
2400
2600
2800
3000
3200
Sigma (%)
4
3
2
1
0
2400
2600
2800
3000
3200
Wavelength

Fig 10

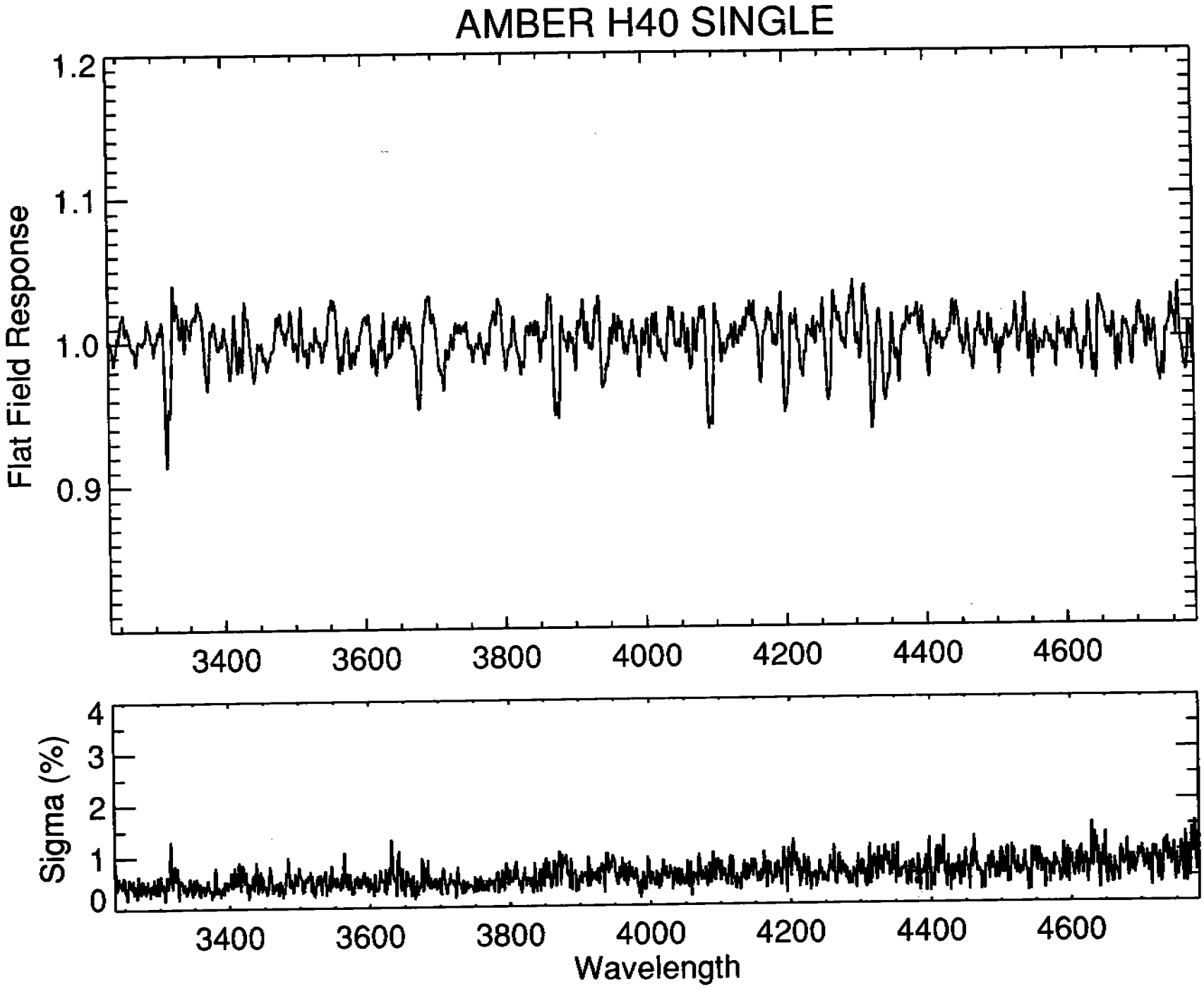
AMBER H40 SINGLE
Flat Field Response
1.2
1.1
1.0
0.9
3400
3600
3800
4000
4200
4400
4600
Sigma (%)
4
3
2
1
0
3400
3600
3800
4000
4200
4400
4600
Wavelength

Fig. 11

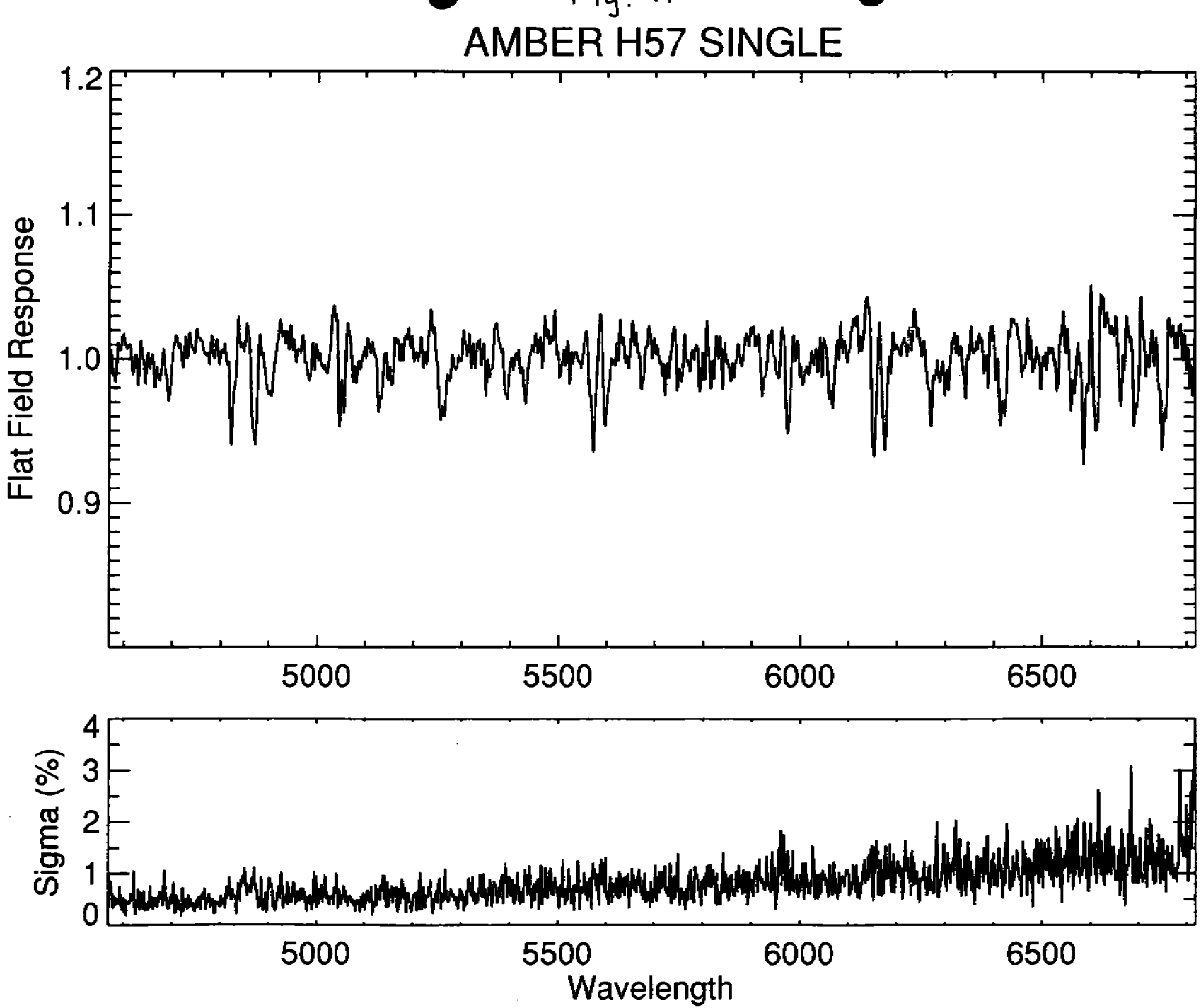
AMBER H57 SINGLE
Flat Field Response
1.2
1.1
1.0
0.9
5000
5500
6000
6500
Sigma (%)
4
3
2
1
0
5000
5500
6000
6500
Wavelength

Fig. 12

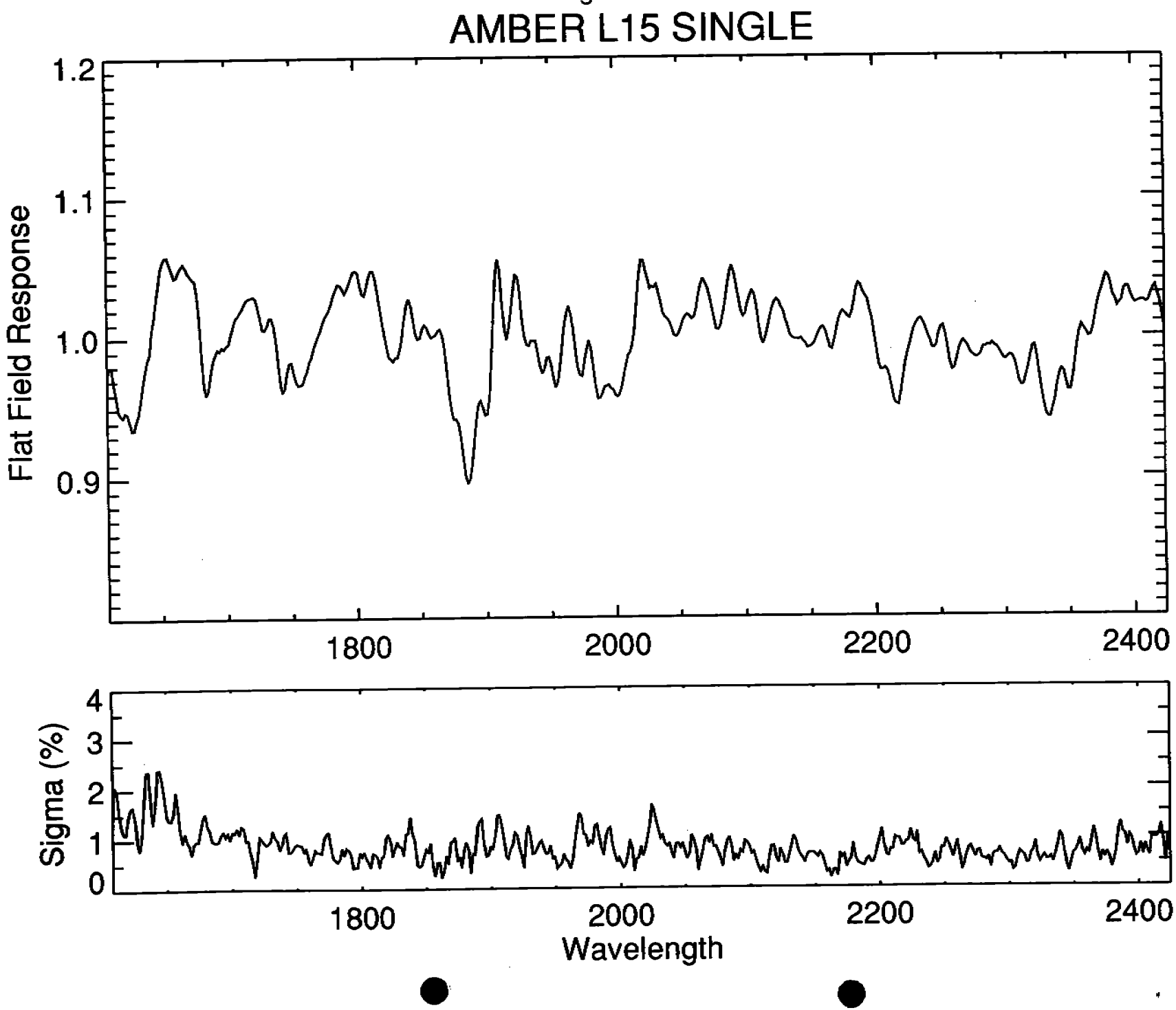
AMBER L15 SINGLE
Flat Field Response
1.2
1.1
1.0
0.9
1800
2000
2200
2400
Sigma (%)
4
3
2
1
0
1800
2000
2200
2400
Wavelength

Fig. 13

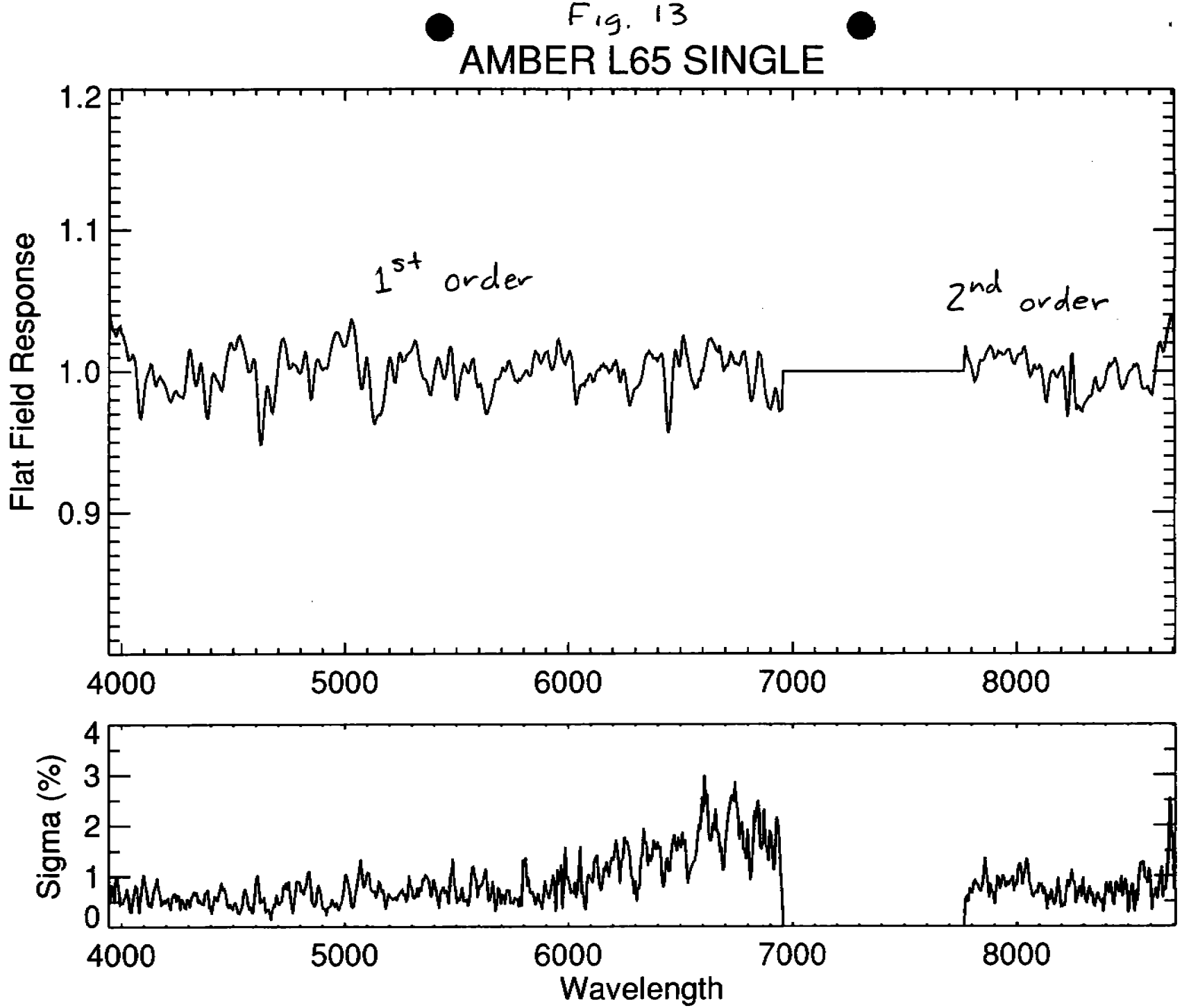
AMBER L65 SINGLE
Flat Field Response
1.2
1.1
1.0
0.9
1st order
2nd order
4000
5000
6000
7000
8000
Sigma (%)
4
3
2
1
0
4000
5000
6000
7000
8000
Wavelength

Fig. 14

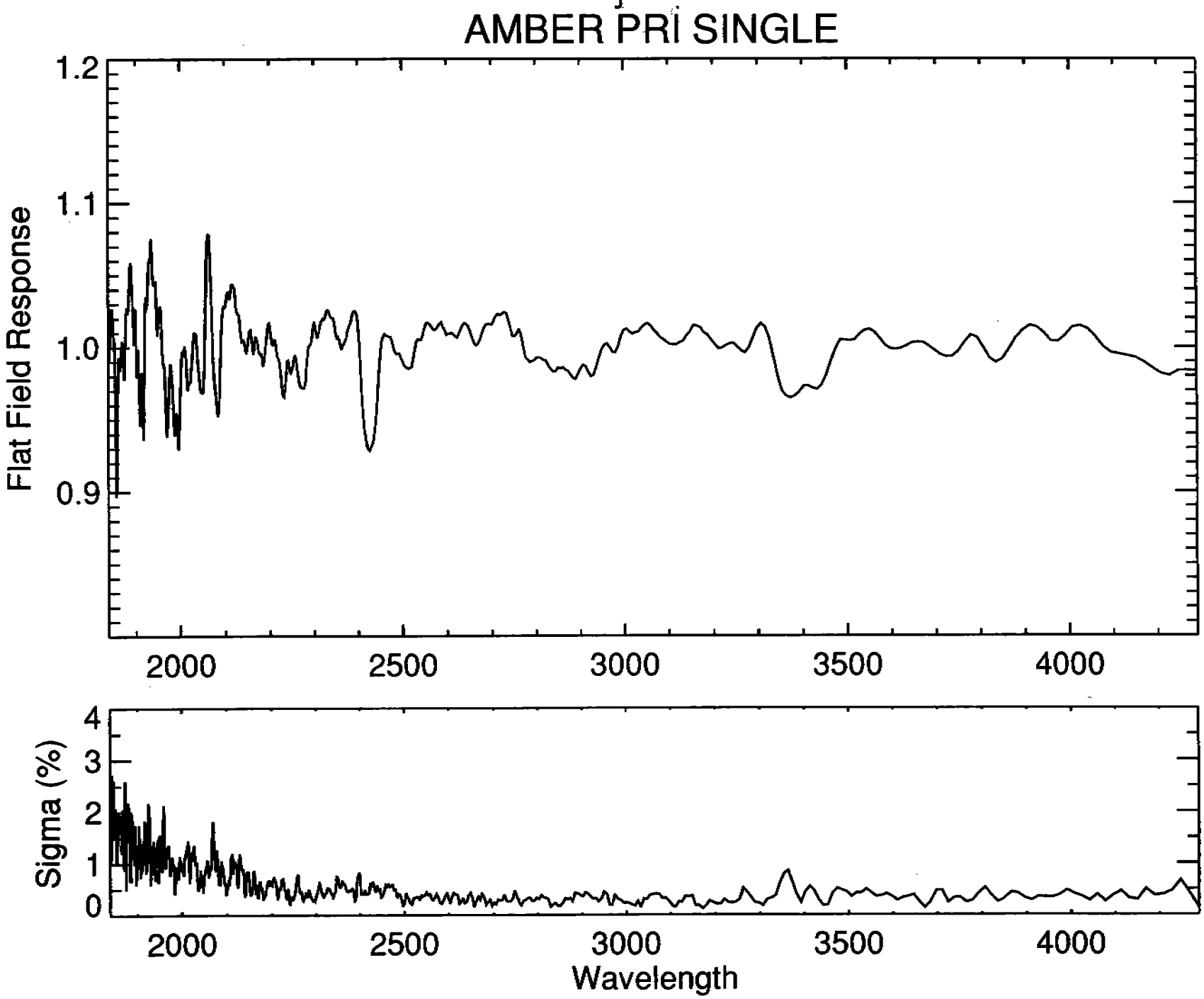
AMBER PRI SINGLE
Flat Field Response
1.2
1.1
1.0
0.9
2000
2500
3000
3500
4000
Sigma (%)
4
3
2
1
0
2000
2500
3000
3500
4000
Wavelength

Fig. 15

Red H19
Flat Field Response

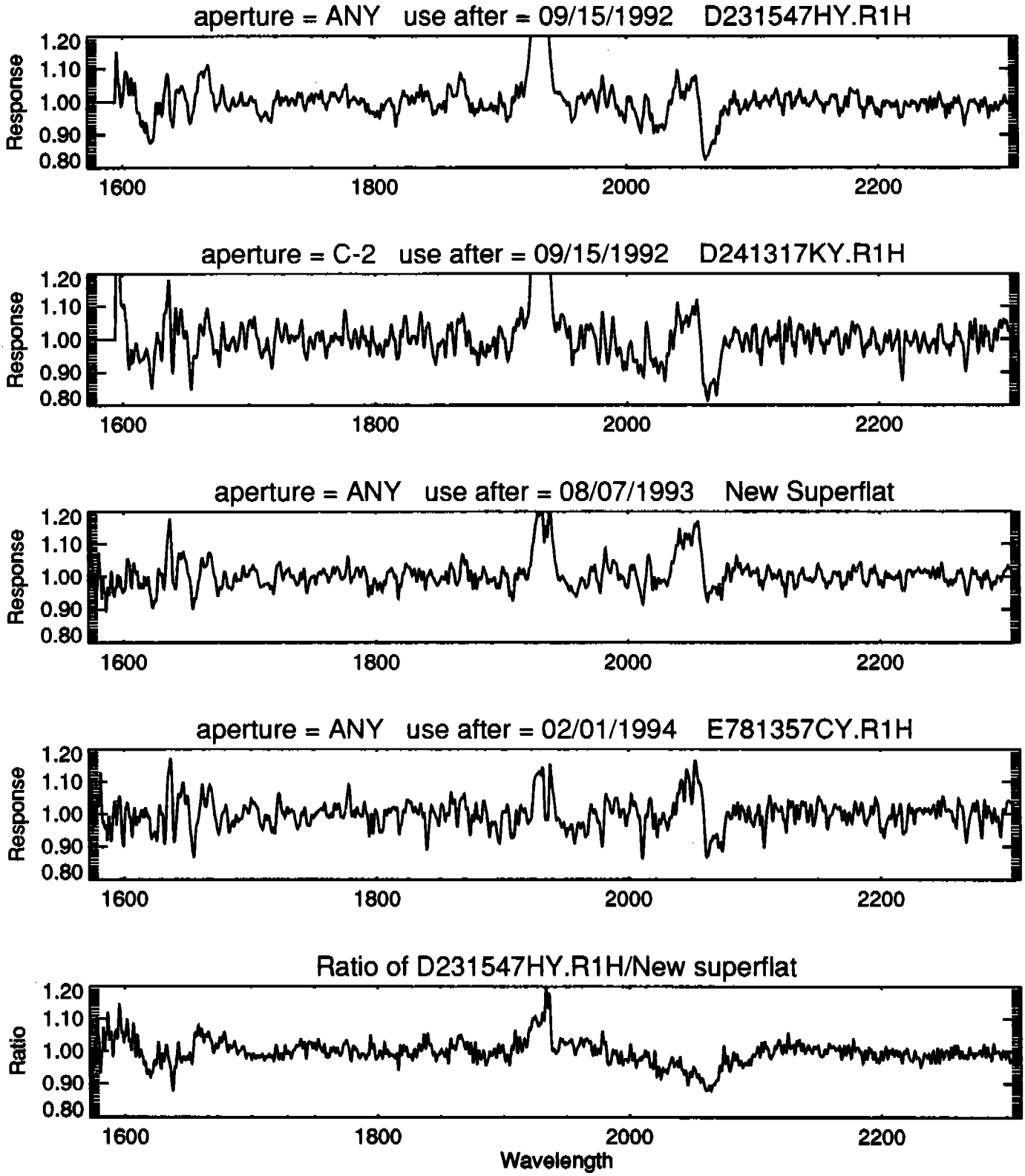

Fig. 16

Red H27
Flat Field Response

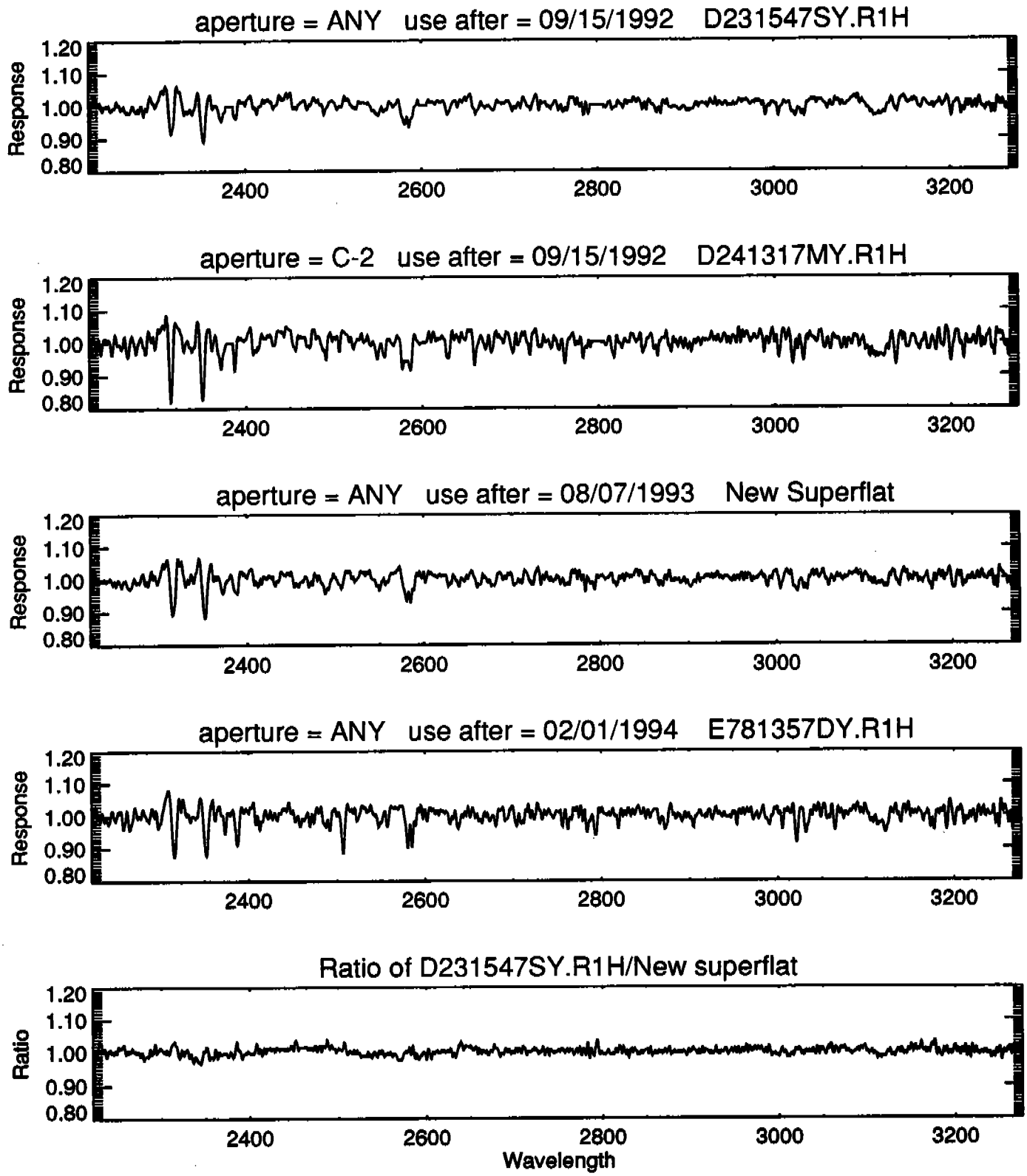

Fig. 17.

Red H40
Flat Field Response

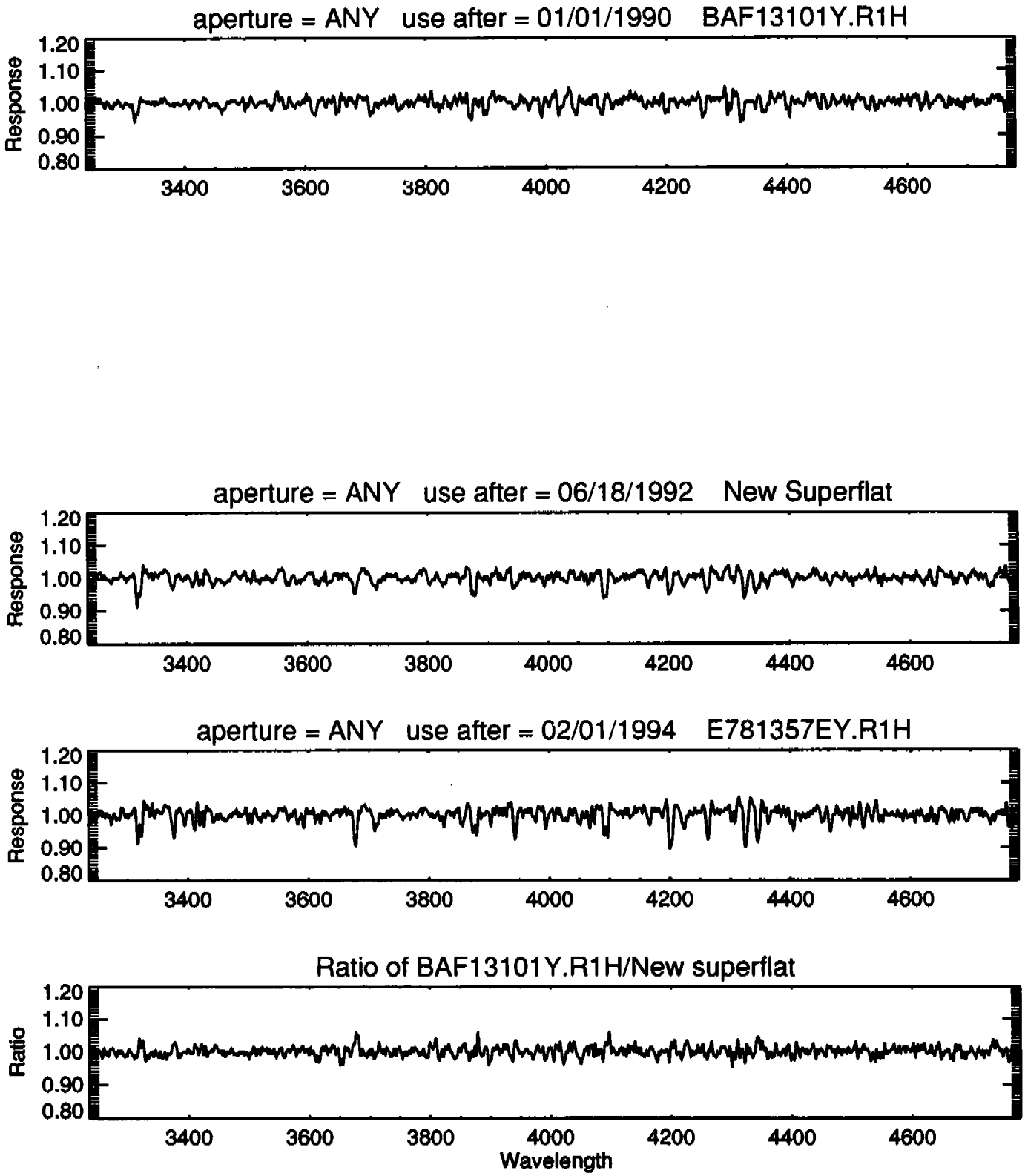

Fig. 18

Red H57
Flat Field Response

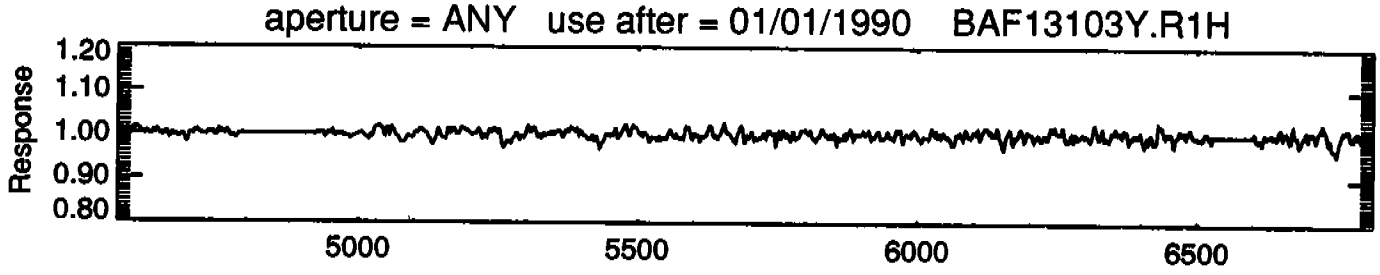

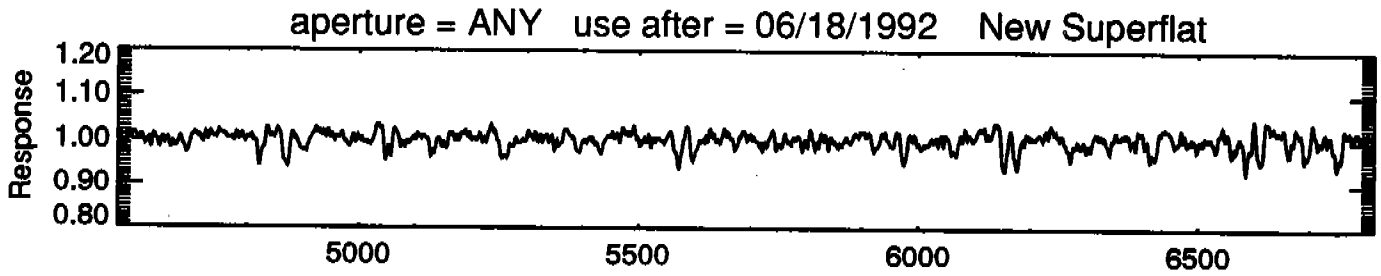

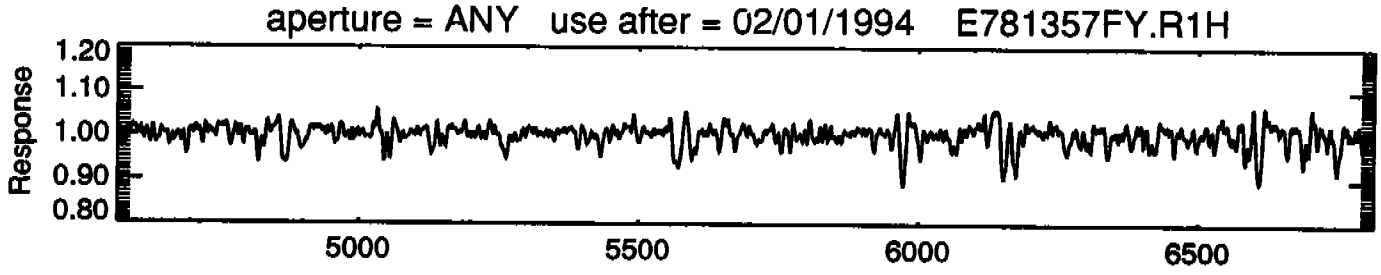

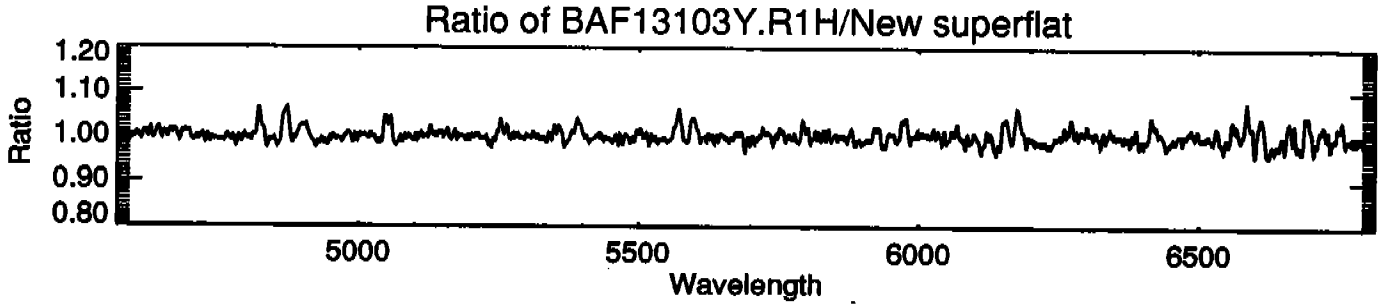

Fig. 19

Red L15
Flat Field Response

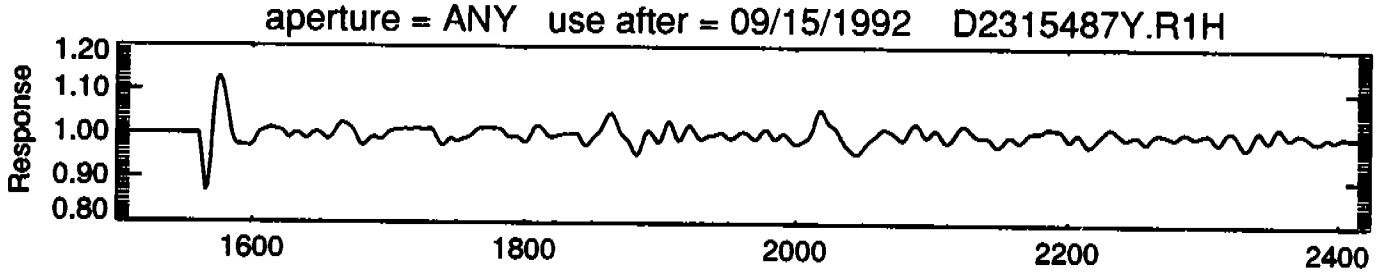

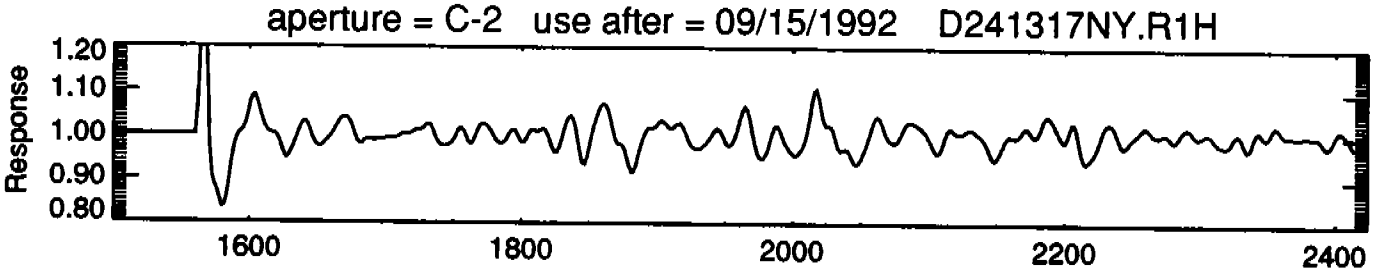

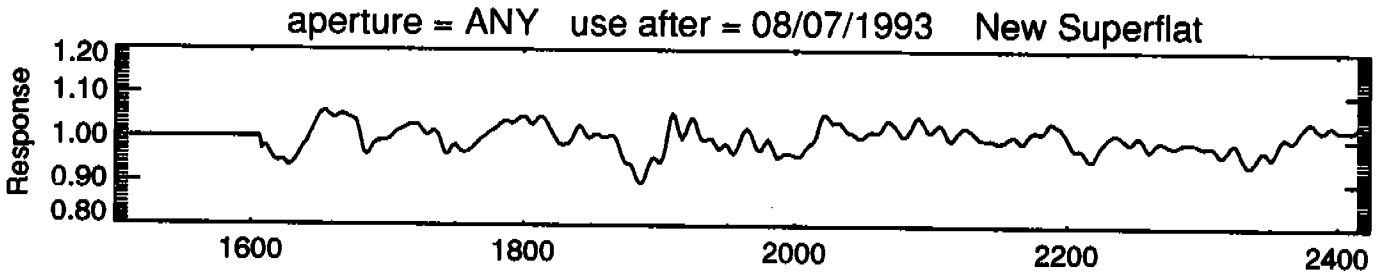

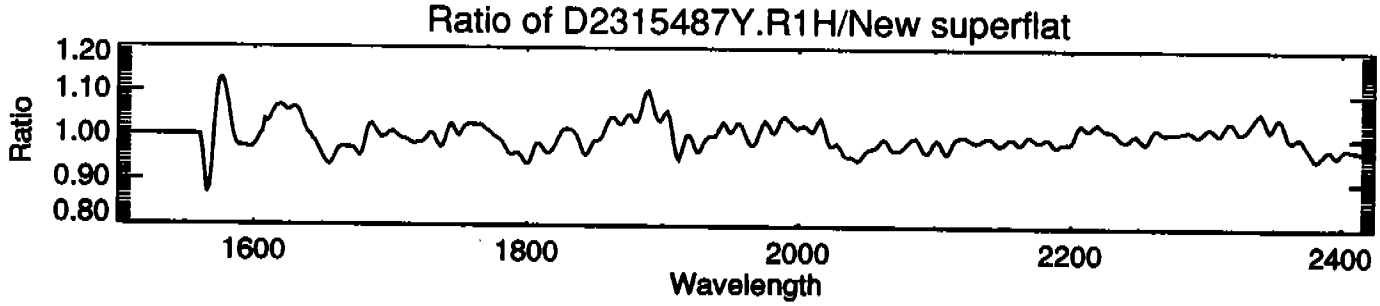

Fig. 20

Red L65
Flat Field Response

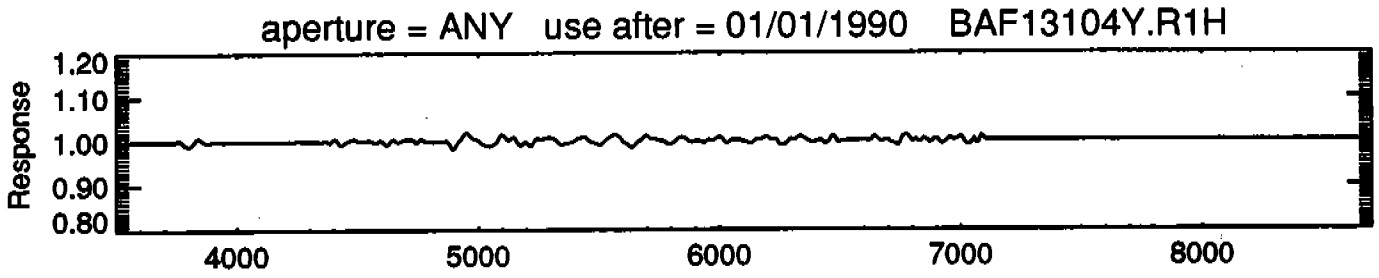

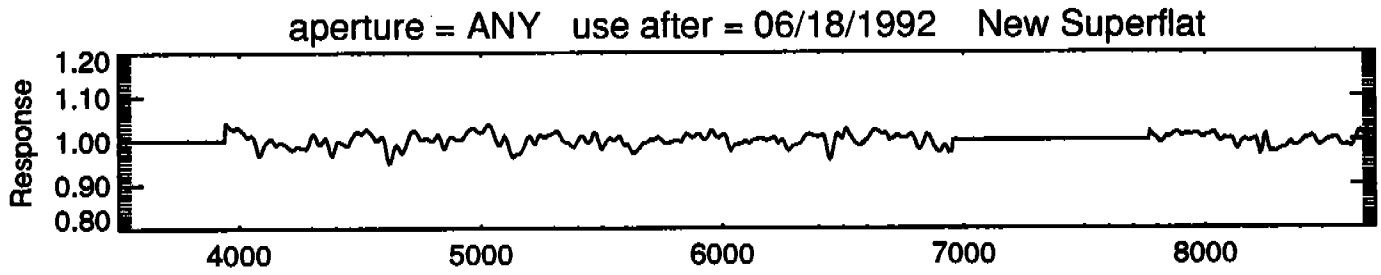

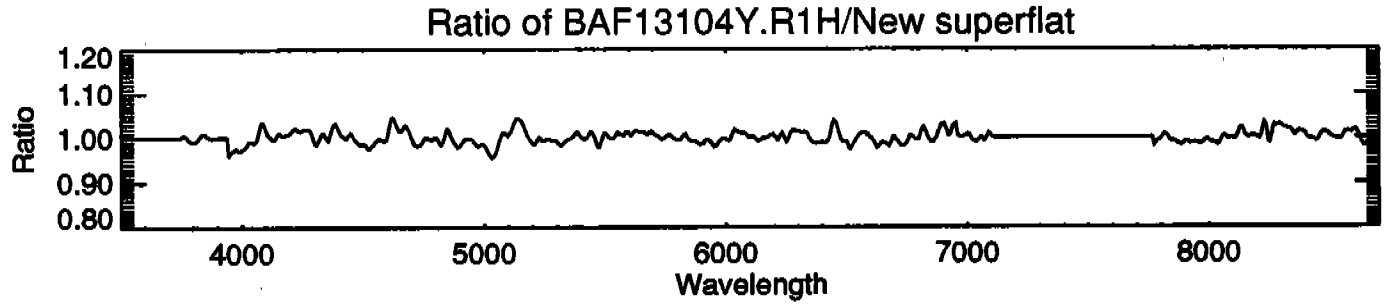

Fig. 21

Red PRI
Flat Field Response